NONLOCAL PERIMETERS AND CURVATURE FLOWS ON GRAPHS WITH APPLICATIONS IN IMAGE PROCESSING AND HIGH-DIMENSIONAL DATA CLASSIFICATION

Imad El Bouchairi, Abderrahim Elmoataz, Jalal M. Fadili

HAL Id: hal-03631338

https://hal.archives-ouvertes.fr/hal-03631338v2

Preprint submitted on 20 Jun 2022

Nonlocal perimeters and curvature flows on graphs with applications in image processing and high-dimensional data classification

Imad El Bouchairi*   Abderrahim Elmoataz*   Jalal Fadili*

June 20, 2022

Abstract. In this paper, we revisit the notion of perimeter on graphs, introduced in [19], and we extend it to so-called inner and outer perimeters. We will also extend the notion of total variation on graphs. Thanks to the co-area formula, we show that discrete total variations can be expressed through these perimeters. Then, we propose a novel class of curvature operators on graphs that unifies both local and nonlocal mean curvature on an Euclidean domain. This leads us to translate and adapt the notion of the mean curvature flow on graphs as well as the level set mean curvature, which can be seen as approximate schemes. Finally, we exemplify the usefulness of these methods in image processing, 3D point cloud processing, and high dimensional data classification.

Key words. Perimeter, total variation, graph cuts, mean curvature flow, image processing, data clustering, PdE on graph, data clustering.

AMS subject classifications. 68Q25, 68R10, 68U05

1 Introduction

1.1 Context and motivations

Partial Differential Equations (PDEs) and variational methods involving the notion of perimeter and curvature have and still generate a lot of interest in both continuous and discrete domains. These notions under their different local or nonlocal forms, arise not only from subfields within mathematics such as differential geometry and analysis, but also in numerous PDEs and objective functionals related to many applications fields in science and engineering.

For instance, in mathematical image processing and computer vision, the notion of perimeter is a key idea for regularizing many ill-posed inverse problems such as denoising, restoration, inpainting, classification, segmentation, etc. Regularizing such problems is often used to find suitable clusters among data, to obtain image partitions for segmentation purposes, to denoise or to inpaint images while preserving sharp boundaries. It is worth noting that perimeters appear in two popular variational models for image processing, namely the total variation and the Mumford-Shah models [14, 32, 30]

---

*Normandie Univ, ENSICAEN, UNICAEN, CNRS, GREYC, France. E-mail: imad.elbouchairi@gmail.com, abderrahim.elmoataz-billah@unicaen.fr, Jalal.Fadili@ensicaen.fr

Motion by mean curvature and geometric flows involving mean curvature play an important role in geometry and analysis. Many models on the continuum, involving a front propagation with a velocity depending on the mean curvature and their simulations by level set methods, are used in different application fields such as data processing, computer vision, fluid mechanics. For an overview and applications see the books [34, 31, 10] and references therein.

In the recent mathematical literature, nonlocal counterparts of the classical local perimeters and curvature flows have been intensively studied. A notion of fractional perimeter and nonlocal curvature was first introduced in [11]. The main idea of fractional perimeters is that any point inside an Euclidean set "interact" with any point outside the set, given a functional whose minimization is taken into account. Many works have then been proposed to study functional minimization involving nonlocal perimeters or nonlocal curvature flows, see e.g. [1, 13] and the recent monograph [28]. In [29], the authors introduce the concepts of perimeter and mean curvature for subsets of a metric random walk space which unify into a broad framework those notions on locally finite weighted connected graphs, those determined by finite Markov chains and some nonlocal evolution problems.

Finite graphs and networks have been widely and successfully used in a variety of fields such as machine learning, data mining, image analysis and social sciences where one is facing analysis and modelling of high dimensional unstructured datasets. In this context, extending the models and methods from variational methods and PDEs to solve problems on graphs is an active research area; see [40, 8, 21, 22] and references therein. Many of these problems, such as classification, clustering or segmentation, can be often formulated in terms of minimizing a graph perimeter (graph cut) or a related functional (normalized cut, ratio cut, balanced cut, etc.). The cut size is, in this case, generally defined as the sum of the weights of edges between the considered set and its complement, which turns out to be closely related to the notion of perimeter of a set on a graph. Such problems on graphs are traditionally solved by methods from combinatorial optimization, graph theory or spectral analysis [24, 35, 37, 42, 9].

1.2 Contributions

Our chief goal on this paper is to formulate and solve different PDEs on weighted graphs involving new discrete graph notions of total variation, perimeter and mean curvature. For this purpose, we adopt nonlocal calculus on weighted graphs, see e.g. [21, 20, 22], which consists in replacing continuous partial differential operators (e.g. gradient, divergence), with reasonable nonlocal discrete analogues. This in turn allows to transfer many important tools and results from the continuous setting to the discrete graph one. Based on this framework, we revisit and extend the discrete notions of perimeter, mean curvature, Cheeger cut and total variation, which lead us to adapt level set equations to weighted graphs. This is illustrated on a variety of applications ranging from data filtering to clustering and segmentation.

1.3 Outline of the paper

In Section 2 we start by reviewing some basic notations and recalling some preliminary material necessary to our exposition. In Section 3, we revisit the notion of boundary sets on graphs as well as discrete perimeters on graphs. In Section 4, we prove an analogue version of the co-area formula on weighted graphs which allows us to derive relation between p-total variation and perimeters on graphs. Equipped with these results, we introduce in Section 5 a family of

mean curvature flows on graphs. We then propose in Section 6 a novel class of mean curvature level set equations on general weighted graphs. Finally, we exemplify the versatility and wide applicability of our framework on several problems in data processing.

2   Notations and preliminaries

2.1   Basics on functions on graphs

All graphs we deal with in this paper are finite undirected graphs. A *weighted graph* $G = (V, E, \omega)$ consists of a finite set V of $N \in \mathbb{N}$ vertices or nodes, a finite set $E \subseteq V \times V$ of edges, and a (symmetric) weight function $\omega : V \times V \to [0, 1]$. The weight of an edge (u, v) is denoted by ω_{uv} is a measure of similarity between the vertices u and v, with the convention $\omega_{uv} = 0$ whenever $v \notin \mathcal{N}(u)$. Here, $\mathcal{N}(u)$ denotes the neighborhood of a vertex u, that is the set of vertices adjacent to u. In the following, we adopt the notation $u \sim v$ to denote two adjacent vertices (i.e., $(u, v) \in E$). The degree $\delta(u)$ of a vertex $u \in V$ is defined as $\delta(u) = \sum_{v \sim u} \sqrt{\omega_{uv}}$.

Throughout this paper, for a subset $\mathcal{A}$ of V, $\mathcal{A}^c \stackrel{\text{def}}{=} V \setminus \mathcal{A}$ is its complement in V, and $\chi_{\mathcal{A}} : V \to \{0, 1\}$ is the characteristic function of $\mathcal{A}$ which takes 1 on $\mathcal{A}$ and 0 otherwise.

Let $G = (V, E, \omega)$ be a weighted graph. We denote by $\mathcal{H}(V)$ the space of real-valued functions on the vertices of G, i.e., each function $f : V \to \mathbb{R}$ in $\mathcal{H}(V)$ assigns a real value $f(u)$ to each vertex $u \in V$.

For a function $f \in \mathcal{H}(V)$ the $\ell^p(V)$-norm of f is

$$\left\| f \right\|_p = \left(\sum_{u \in V} \left| f(u) \right|^p \right)^{\frac{1}{p}} \quad \text{for} \quad 1 \leqslant p < \infty, \ \text{and} \ \left\| f \right\|_\infty = \max_{u \in V} \left| f(u) \right|.$$

The space $\mathcal{H}(V)$ endowed with the inner product $\langle f, g \rangle_{\mathcal{H}(V)} = \sum_{u \in V} f(u)g(u)$, $f, g \in \mathcal{H}(V)$, is a Hilbert space. Similarly, let $\mathcal{H}(E)$ be the space of real-valued functions defined on the edges of the graph, i.e., each function $H : E \to \mathbb{R}$ in $\mathcal{H}(E)$ assigns a real value $H(u, v)$ to each edge $(u, v) \in E$. The space $\mathcal{H}(E)$ endowed with the inner product $\langle H, F \rangle_{\mathcal{H}(E)} = \sum_{(u,v) \in E} H(u, v)F(u, v)$, $H, F \in \mathcal{H}(E)$, is a Hilbert space.

2.2   Partial difference operators on graphs

Let us recall some weighted partial difference operators on graphs that are essential in our paper. We refer to [21, 23, 38, 20], for more detailed description of these operators.

The *weighted finite difference operator* of a function $f \in \mathcal{H}(V)$, denoted by $\mathbf{d}_\omega : \mathcal{H}(V) \to \mathcal{H}(E)$, is defined on a pair of vertices $(u, v) \in E$ as:

$$\mathbf{d}_\omega f(u, v) = \sqrt{\omega_{uv}}(f(v) - f(u)).$$

Note that this difference operator is linear and antisymmetric.

The adjoint of the difference operator $\mathbf{d}_\omega$ is the linear operator $\mathbf{d}_\omega^* : \mathcal{H}(E) \to \mathcal{H}(V)$ verifying $\langle \mathbf{d}_\omega f, H \rangle_{\mathcal{H}(E)} = \langle f, \mathbf{d}_\omega^* H \rangle_{\mathcal{H}(V)}$ for all $f \in \mathcal{H}(V)$ and $H \in \mathcal{H}(E)$. Using this, it can be easily seen that

$$\mathbf{d}_\omega^* H(u) = \sum_{v \sim u} \sqrt{\omega_{uv}}(H(v, u) - H(u, v)).$$

The *divergence operator* is defined as

$$\mathbf{div}_\omega = -\mathbf{d}_\omega^*.$$

Its action on a function in $\mathcal{H}(E)$ measures the net outflow of the function at each vertex of the graph. Each function $H \in \mathcal{H}(E)$ has a null divergence over the entire set of vertices. Indeed, from the previous definitions, it can be easily shown that $\sum_{u \in V} \sum_{v \sim u} \mathbf{d}_\omega f(u, v) = 0$, for all $f \in \mathcal{H}(V)$, and $\sum_{u \in V} \mathbf{div}_\omega H(u) = 0$, for all $H \in \mathcal{H}(E)$.

We introduce the *weighted gradient* operator on graphs ∇_ω acting on functions on $\mathcal{H}(V)$, which is defined on a vertex $u \in V$ as the vector

$$\nabla_\omega f(u) = (\mathbf{d}_\omega f(u, v))_{v \sim u}.$$

It is clear from the properties of $\mathbf{d}_\omega$ that ∇_ω is linear and antisymmetric. Similarly we define the upwind and downwind weighted gradient operators on graphs $\nabla_\omega^\pm$ as

$$\nabla_\omega^\pm f(u) = (\sqrt{\omega_{uv}} \, (f(v) - f(u))^\pm)_{v \sim u},$$

where $a^+ = \max(a, 0)$ and $a^- = \max(-a, 0)$, $\forall a \in \mathbb{R}$.

For $1 \leq p \leq \infty$, the gradient p-norm is the seminorm $\|\cdot\|_p \circ \nabla_\omega : \mathcal{H}(V) \to (\mathbb{R}^+)^N$ given by

$$\left\|\nabla_\omega f(u)\right\|_p = \begin{cases} \left(\sum_{v \sim u} (\omega_{uv})^{\frac{p}{2}} |f(v) - f(u)|^p\right)^{\frac{1}{p}}, & p \in [1, +\infty[\\ \max_{v \sim u} (\sqrt{\omega_{uv}} |f(v) - f(u)|), & p = +\infty. \end{cases}$$

and likewise for the operator $\nabla_\omega^\pm$ instead of ∇_ω. The integral of a function f in $\mathcal{H}(V)$ (with respect to the empirical measure on V) is denoted by

$$\mathscr{I}(f) = \sum_{u \in V} f(u).$$

3 Generalized perimeters on graphs

3.1 Boundaries on graphs

We start by defining what we intend by a boundary of a subset $\mathcal{A} \subset V$ on an undirected graph.

Definition 3.1. *The* outer *and* inner vertex boundaries *of a subset $\mathcal{A} \subset V$, are respectively defined by*

$$\partial^+ \mathcal{A} \stackrel{\text{def}}{=} \{u \in \mathcal{A}^c : \exists v \in \mathcal{A}, \, v \sim u\}, \tag{3.1}$$

$$\partial^- \mathcal{A} \stackrel{\text{def}}{=} \{u \in \mathcal{A} : \exists v \in \mathcal{A}^c, \, v \sim u\}, . \tag{3.2}$$

The vertex boundary *of $\mathcal{A}$ is the set*

$$\partial \mathcal{A} \stackrel{\text{def}}{=} \partial^+ \mathcal{A} \cup \partial^- \mathcal{A}. \tag{3.3}$$

An immediate consequence of these definitions is that $\partial^+ \mathcal{A}^c = \partial^- \mathcal{A}$, $\partial \mathcal{A} = \partial \mathcal{A}^c$ and $\partial^+ \mathcal{A} \cap \partial^- \mathcal{A} = \emptyset$.

The following proposition gives relationships between the discrete gradients of $\chi_\mathcal{A}$ and the above boundary sets, which will prove useful to define discrete perimeters on graphs. Its proof follows from simple computations and we omit it here for the sake of brevity.

Proposition 3.1. *Let $G = (V, E, w)$ a weighted graph and $\mathcal{A} \subset V$.*

(i) For $1 \leq p < \infty$, we have the following relations:

$$\|\nabla_\omega^+ \chi_\mathcal{A}(u)\|_p = \left(\sum_{v \in \mathcal{A}} (\omega_{uv})^{\frac{p}{2}} \right)^{\frac{1}{p}} \chi_{\partial^+ \mathcal{A}}(u), \tag{3.4}$$

$$\left\|\nabla_\omega^- \chi_\mathcal{A}(u)\right\|_p = \left(\sum_{v \in \mathcal{A}^c} (\omega_{uv})^{\frac{p}{2}} \right)^{\frac{1}{p}} \chi_{\partial^- \mathcal{A}}(u), \tag{3.5}$$

$$\left\|\nabla_\omega \chi_\mathcal{A}(u)\right\|_p = \left\|\nabla_\omega^+ \chi_\mathcal{A}(u)\right\|_p + \left\|\nabla_\omega^- \chi_\mathcal{A}(u)\right\|_p. \tag{3.6}$$

(ii) For $p = \infty$, we have the following relations:

$$\|\nabla_\omega^+ \chi_\mathcal{A}(u)\|_\infty = \left(\max_{v \in \mathcal{A}} \left(\sqrt{\omega_{uv}}\right) \right) \chi_{\partial^+ \mathcal{A}}(u),$$

$$\left\|\nabla_\omega^- \chi_\mathcal{A}(u)\right\|_\infty = \left(\max_{v \in \mathcal{A}^c} \left(\sqrt{\omega_{uv}}\right) \right) \chi_{\partial^- \mathcal{A}}(u),$$

$$\left\|\nabla_\omega \chi_\mathcal{A}(u)\right\|_\infty = \left\|\nabla_\omega^+ \chi_\mathcal{A}(u)\right\|_\infty + \left\|\nabla_\omega^- \chi_\mathcal{A}(u)\right\|_\infty.$$

(iii) Moreover, for $p \in [1, +\infty]$, we have

$$\left\|\nabla_\omega^+ \chi_\mathcal{A}(u)\right\|_p = \left\|\nabla_\omega^- \chi_{\mathcal{A}^c}(u)\right\|_p \ \text{and} \ \left\|\nabla_\omega \chi_\mathcal{A}(u)\right\|_p \qquad = \left\|\nabla_\omega \chi_{\mathcal{A}^c}(u)\right\|_p.$$

Remark 3.1. *For unweighted graphs i.e. $\omega_{uv} \in \{0, 1\}$, the above norms have the following useful meanings:*

- *$\|\nabla_\omega^+ \chi_\mathcal{A}(u)\|_1$ is the number of edges connecting the vertex $u \in \mathcal{A}^c$ with the vertices in $\mathcal{A}$. Therefore $\sum_{u \in V} \left\|\nabla_\omega^+ \chi_\mathcal{A}(u)\right\|_1$ is just the size of the usual edge boundary of $\mathcal{A}$.*

- *$\|(\nabla_\omega^\pm \chi_\mathcal{A})(u)\|_\infty$ coincide with $\chi_{\partial^\pm \mathcal{A}}(u)$, and so $\sum_{u \in V} \left\|\nabla_\omega^+ \chi_\mathcal{A}(u)\right\|_\infty$ (resp. $\sum_{u \in V} \left\|\nabla_\omega^- \chi_\mathcal{A}(u)\right\|_\infty$) is the size of the outer (resp. inner) vertex boundary of $\mathcal{A}$.*

  For weighted graphs i.e. $\omega_{uv} \in [0, 1]$, we observe that $\sum_{u \in V} \left\|\nabla_\omega^+ \chi_\mathcal{A}(u)\right\|_\infty$ (resp. $\sum_{u \in V} \left\|\nabla_\omega^- \chi_\mathcal{A}(u)\right\|_\infty$) is the weighted size of the outer (resp. inner) vertex boundary of $\mathcal{A}$.

Remark 3.2. *The outer and inner vertex boundaries, and the vertex boundary can be equivalently expressed via $\chi_\mathcal{A}$ as:*

$$\partial^+ \mathcal{A} = \left\{ u \in V : \ \left\|\nabla_\omega^+ \chi_\mathcal{A}(u)\right\|_p > 0 \right\},$$

$$\partial^- \mathcal{A} = \left\{ u \in V : \ \left\|\nabla_\omega^- \chi_\mathcal{A}(u)\right\|_p > 0 \right\},$$

$$\partial \mathcal{A} = \left\{ u \in V : \ \left\|\nabla_\omega \chi_\mathcal{A}(u)\right\|_p > 0 \right\}.$$

3.2 Perimeters on graphs

Owing to the interpretation of Proposition 3.1, we recall the definition of the family of weighted perimeters on graphs introduced in [19].

Definition 3.2. *Let* $G = (V, E, \omega)$. *For* $1 \leq p < \infty$ *and* $\mathcal{A} \subset V$, *the family of weighted perimeters of* $\mathcal{A}$ *is defined as follows:*

$$\mathrm{Per}^+_{\omega,p}(\mathcal{A}) \stackrel{\mathrm{def}}{=} \mathscr{I}(\|\nabla^+_w \chi_{\mathcal{A}}(\cdot)\|_p) = \sum_{u \in \mathcal{A}^c} \left(\sum_{v \in \mathcal{A}} \omega_{uv}^{\frac{p}{2}} \right)^{\frac{1}{p}},$$

$$\mathrm{Per}^-_{\omega,p}(\mathcal{A}) \stackrel{\mathrm{def}}{=} \mathscr{I}(\|\nabla^-_\omega \chi_{\mathcal{A}}(\cdot)\|_p) = \sum_{u \in \mathcal{A}} \left(\sum_{v \in \mathcal{A}^c} \omega_{uv}^{\frac{p}{2}} \right)^{\frac{1}{p}},$$

$$\mathrm{Per}_{\omega,p}(\mathcal{A}) \stackrel{\mathrm{def}}{=} \mathscr{I}(\|\nabla_\omega \chi_{\mathcal{A}}(\cdot)\|_p) = \sum_{u \in \mathcal{A}^c} \left(\sum_{v \in \mathcal{A}} \omega_{uv}^{\frac{p}{2}} \right)^{\frac{1}{p}} + \sum_{u \in \mathcal{A}} \left(\sum_{v \in \mathcal{A}^c} \omega_{uv}^{\frac{p}{2}} \right)^{\frac{1}{p}}.$$

For $p = \infty$, *the family of weighted perimeters of* $\mathcal{A} \subset V$ *is defined as follows:*

$$\mathrm{Per}^+_{\omega,\infty}(\mathcal{A}) \stackrel{\mathrm{def}}{=} \mathscr{I}(\|\nabla^+_\omega \chi_{\mathcal{A}}(\cdot)\|_\infty) = \sum_{u \in \mathcal{A}^c} \left(\max_{v \in \mathcal{A}} \sqrt{\omega_{uv}} \right),$$

$$\mathrm{Per}^-_{\omega,\infty}(\mathcal{A}) \stackrel{\mathrm{def}}{=} \mathscr{I}(\|\nabla^-_\omega \chi_{\mathcal{A}}(\cdot)\|_\infty) = \sum_{u \in \mathcal{A}} \left(\max_{v \in \mathcal{A}^c} \sqrt{\omega_{uv}} \right),$$

$$\mathrm{Per}_{\omega,\infty}(\mathcal{A}) \stackrel{\mathrm{def}}{=} \mathscr{I}(\|\nabla_\omega \chi_{\mathcal{A}}(\cdot)\|_\infty) = \sum_{u \in \mathcal{A}^c} \left(\max_{v \in \mathcal{A}} \sqrt{\omega_{uv}} \right) + \sum_{u \in \mathcal{A}} \left(\max_{v \in \mathcal{A}^c} \sqrt{\omega_{uv}} \right).$$

It is clear from the definition above that, for $1 \leq p \leq \infty$,

$$\mathrm{Per}_{\omega,p}(\mathcal{A}) = \mathrm{Per}^+_{\omega,p}(\mathcal{A}) + \mathrm{Per}^-_{\omega,p}(\mathcal{A}), \quad \mathrm{Per}_{\omega,p}(\mathcal{A}) = \mathrm{Per}_{\omega,p}(\mathcal{A}^c),$$

$$\mathrm{Per}^+_{\omega,p}(\mathcal{A}) = \mathrm{Per}^-_{\omega,p}(\mathcal{A}^c), \quad \mathrm{Per}^+_{\omega,1}(\mathcal{A}) = \mathrm{Per}^-_{\omega,1}(\mathcal{A}) \text{ and } \mathrm{Per}_{\omega,1}(\mathcal{A}) = 2\,\mathrm{Per}^\pm_{\omega,1}(\mathcal{A}).$$

Proposition 3.2. *Let* $p \in \{1, +\infty\}$ *and* P_ω *belongs to* $\{\mathrm{Per}^\pm_{\omega,p}, \mathrm{Per}_{\omega,p}\}$. *In the case* $p = \infty$, *we assume that the graph is unweighted, i.e.,* ω *is* $\{0, 1\}$-*valued. We have the following properties:*

(i) $P_\omega(\emptyset) = 0$;

(ii) $P_\omega(V) = 0$;

(iii) P_ω *is submodular, i.e., for all* $\mathcal{A}, \mathcal{B} \subset V$ *we have*

$$P_\omega(\mathcal{A} \cup \mathcal{B}) + P_\omega(\mathcal{A} \cap \mathcal{B}) \leq P_\omega(\mathcal{A}) + P_\omega(\mathcal{B}).$$

PROOF : Claims (i) and (ii) are straightforward. We thus focus on claim (iii).

For $p = 1$, it is enough to prove the inequality for $\mathrm{Per}^+_{\omega,1}$ since $\mathrm{Per}_{\omega,1}(\mathcal{A}) = 2\,\mathrm{Per}^+_{\omega,1}(\mathcal{A})$. We have

$$\mathrm{Per}^+_{\omega,1}(\mathcal{A} \cup \mathcal{B}) = \sum_{u \in \mathcal{A} \cup \mathcal{B}} \sum_{v \in (\mathcal{A} \cup \mathcal{B})^c} \sqrt{\omega_{uv}}$$

$$= \sum_{u \in \mathcal{A}} \sum_{v \in \mathcal{A}^c} \sqrt{\omega_{uv}} + \sum_{u \in \mathcal{B}} \sum_{v \in \mathcal{B}^c} \sqrt{\omega_{uv}} - \sum_{u \in \mathcal{A} \cap \mathcal{B}} \sum_{v \in (\mathcal{A} \cup \mathcal{B})^c} \sqrt{\omega_{uv}}$$
$$- \sum_{u \in \mathcal{A}} \sum_{v \in \mathcal{B} \setminus (\mathcal{A} \cup \mathcal{B})^c} \sqrt{\omega_{uv}} - \sum_{u \in \mathcal{B}} \sum_{v \in \mathcal{A} \setminus (\mathcal{A} \cup \mathcal{B})^c} \sqrt{\omega_{uv}},$$

and

$$\mathrm{Per}_{\omega,1}^{+} (\mathcal{A} \cap \mathcal{B}) = \sum_{u \in \mathcal{A} \cap \mathcal{B}} \sum_{v \in (\mathcal{A} \cap \mathcal{B})^c} \sqrt{\omega_{uv}}$$
$$= \sum_{u \in \mathcal{A} \cap \mathcal{B}} \sum_{v \in (\mathcal{A} \cup \mathcal{B})^c} \sqrt{\omega_{uv}} + \sum_{u \in \mathcal{A} \cap \mathcal{B}} \sum_{v \in \mathcal{A} \setminus (\mathcal{A} \cup \mathcal{B})^c} \sqrt{\omega_{uv}}$$
$$+ \sum_{u \in \mathcal{A} \cap \mathcal{B}} \sum_{v \in \mathcal{B} \setminus (\mathcal{A} \cup \mathcal{B})^c} \sqrt{\omega_{uv}}.$$

Adding these two equalities we get

$$\mathrm{Per}_{\omega,1}^{+} (\mathcal{A} \cup \mathcal{B}) + \mathrm{Per}_{\omega,1}^{+} (\mathcal{A} \cap \mathcal{B}) = \sum_{u \in \mathcal{A}} \sum_{v \in \mathcal{A}^c} \sqrt{\omega_{uv}} + \sum_{u \in \mathcal{B}} \sum_{v \in \mathcal{B}^c} \sqrt{\omega_{uv}}$$
$$- \left(\sum_{u \in \mathcal{B}} \sum_{v \in \mathcal{A} \setminus (\mathcal{A} \cup \mathcal{B})^c} \sqrt{\omega_{uv}} - \sum_{u \in \mathcal{A} \cap \mathcal{B}} \sum_{v \in \mathcal{A} \setminus (\mathcal{A} \cup \mathcal{B})^c} \sqrt{\omega_{uv}} \right)$$
$$- \left(\sum_{u \in \mathcal{A}} \sum_{v \in \mathcal{B} \setminus (\mathcal{A} \cup \mathcal{B})^c} \sqrt{\omega_{uv}} - \sum_{u \in \mathcal{A} \cap \mathcal{B}} \sum_{v \in \mathcal{B} \setminus (\mathcal{A} \cup \mathcal{B})^c} \sqrt{\omega_{uv}} \right)$$
$$\leq \sum_{u \in \mathcal{A}} \sum_{v \in \mathcal{A}^c} \sqrt{\omega_{uv}} + \sum_{u \in \mathcal{B}} \sum_{v \in \mathcal{B}^c} \sqrt{\omega_{uv}}$$
$$= \mathrm{Per}_{\omega,1}^{+} (\mathcal{A}) + \mathrm{Per}_{\omega,1}^{+} (\mathcal{B}).$$

For $\mathrm{Per}_{\omega,\infty}^{\pm}$, claim (iii) is a consequence of the following inequality, which is easy to verify,

$$\max_{v \sim u} (\chi_{\mathcal{A} \cup \mathcal{B}}(v) - \chi_{\mathcal{A} \cup \mathcal{B}}(u))^{\pm} + \max_{v \sim u} (\chi_{\mathcal{A} \cap \mathcal{B}}(v) - \chi_{\mathcal{A} \cap \mathcal{B}}(u))^{\pm}$$
$$\leq \max_{v \sim u} (\chi_{\mathcal{A}}(v) - \chi_{\mathcal{A}}(u))^{\pm} + \max_{v \sim u} (\chi_{\mathcal{B}}(v) - \chi_{\mathcal{B}}(u))^{\pm},$$

for all $u \in V$. I turn, the result holds for $\mathrm{Per}_{\omega,\infty}$ since $\mathrm{Per}_{\omega,\infty} = \mathrm{Per}_{\omega,\infty}^{+} + \mathrm{Per}_{\omega,\infty}^{-}$ by definition.
$\square$

As a consequence of Proposition 3.2, we have the following result for $p = 1$.

Corollary 3.1. *Let $\mathcal{A}$, $\mathcal{B} \subset V$ with $\mathcal{A} \cap \mathcal{B} = \emptyset$, then*

$$\mathrm{Per}_{\omega,1}^{\pm}(\mathcal{A} \cup \mathcal{B}) = \mathrm{Per}_{\omega,1}^{\pm}(\mathcal{A}) + \mathrm{Per}_{\omega,1}^{\pm}(\mathcal{B}) - 2 \sum_{u \in \mathcal{A}} \sum_{v \in \mathcal{B}} \sqrt{\omega_{uv}},$$
$$\mathrm{Per}_{\omega,1}(\mathcal{A} \cup \mathcal{B}) = \mathrm{Per}_{\omega,1}(\mathcal{A}) + \mathrm{Per}_{\omega,1}(\mathcal{B}) - 4 \sum_{u \in \mathcal{A}} \sum_{v \in \mathcal{B}} \sqrt{\omega_{uv}}.$$

If moreover, there are no edges between $\mathcal{A}$ and $\mathcal{B}$, i.e., $\partial\mathcal{A} \cap \mathcal{B} = \emptyset$ or equivalently $\partial\mathcal{B} \cap \mathcal{A} = \emptyset$, then

$$\mathrm{Per}_{\omega,1}^{\pm}(\mathcal{A} \cup \mathcal{B}) = \mathrm{Per}_{\omega,1}^{\pm}(\mathcal{A}) + \mathrm{Per}_{\omega,1}^{\pm}(\mathcal{B}),$$
$$\mathrm{Per}_{\omega,1}(\mathcal{A} \cup \mathcal{B}) = \mathrm{Per}_{\omega,1}(\mathcal{A}) + \mathrm{Per}_{\omega,1}(\mathcal{B}).$$

PROOF :   We prove the claims for $\mathrm{Per}_{\omega,1}$, those for $\mathrm{Per}_{\omega,1}^{\pm}$ follow from the fact that $\mathrm{Per}_{\omega,1}(\mathcal{A})^{\pm} = \frac{1}{2}\mathrm{Per}_{\omega,1}(\mathcal{A})$. By definition, we have

$$
\begin{aligned}
\mathrm{Per}_{\omega,1}(\mathcal{A} \cup \mathcal{B}) &= \sum_{u \in V}\sum_{v \in V}\sqrt{\omega_{uv}}\left(\chi_{\mathcal{A}\cup\mathcal{B}}(v) - \chi_{\mathcal{A}\cup\mathcal{B}}(u)\right)^2 \\
&= \sum_{u \in V}\sum_{v \in V}\sqrt{\omega_{uv}}\left(\chi_{\mathcal{A}}(v) + \chi_{\mathcal{B}}(v) - \chi_{\mathcal{A}}(u) - \chi_{\mathcal{B}}(u)\right)^2 \\
&= \sum_{u \in V}\sum_{v \in V}\sqrt{\omega_{uv}}\left(\chi_{\mathcal{A}}(v) - \chi_{\mathcal{A}}(u)\right)^2 + \sum_{u \in V}\sum_{v \in V}\sqrt{\omega_{uv}}\left(\chi_{\mathcal{B}}(v) - \chi_{\mathcal{B}}(u)\right)^2 \\
&\qquad + 2\sum_{u \in V}\sum_{v \in V}\sqrt{\omega_{uv}}\left(\chi_{\mathcal{A}}(v) - \chi_{\mathcal{A}}(u)\right)\left(\chi_{\mathcal{B}}(v) - \chi_{\mathcal{B}}(u)\right) \\
&= \mathrm{Per}_{\omega,1}(\mathcal{A}) + \mathrm{Per}_{\omega,1}(\mathcal{B}) - 4\sum_{\mathcal{A}}\sum_{\mathcal{B}}\sqrt{\omega_{uv}}.
\end{aligned}
$$

$\square$

Remark 3.3 (Continuum limits). *There has been much interest in recent years in introducing notions of nonlocal perimeter in terms of nonlocal functionals on the continuum and the study of their convergence to the local perimeter (in the sense of De Giorgi). Related works can be found in [5, 16, 7, 4, 12, 28]. One may then wonder whether our perimeter on graphs $\mathrm{Per}_{\omega,1}$ has a nonlocal (resp. local) continuum limit as the number of vertices grows to infinity (resp. and appropriately rescaling the weight function ω). Characterizing such a limit, the corresponding convergence rate, as well as the relation of this limit to the functionals defined in the above-cited papers would in turn shed light on consistency of $\mathrm{Per}_{\omega,1}$ as a discrete graph-based estimator of the perimeter. These are crucial and nontrivial questions that are beyond the scope of this paper and that we propose to investigate in a future work.*

4   Generalized p-total variation on graphs

In this section, we extend the notion of total variation, for $p = 1$, on graphs to upwind and downwind p-total variations and also for $p \in [1, \infty]$. We show that the result of the co-area formula provided in [19, 40] is still valid for $p = \infty$ on unweighted graphs.

Definition 4.1. *Let $G = (V, E, \omega)$. For $1 \le p < \infty$, the p-total variation of $f : V \to \mathbb{R}$ and its upwind and downwind versions are defined as follows:*

$$\mathrm{TV}_{\omega,p}(f) = \mathscr{I}\left(\left\|\nabla_{\omega}f(\cdot)\right\|_p\right) = \sum_{u \in V}\left(\sum_{v \in V}\omega_{uv}^{\frac{p}{2}}\left|f(v) - f(u)\right|^p\right)^{\frac{1}{p}}$$

8

$$\mathrm{TV}^{\pm}_{\omega,p}(f) = \mathscr{I}\left(\left\|\nabla^{\pm}_{\omega}f(\cdot)\right\|_p\right) = \sum_{u \in V}\left(\sum_{v \in V}\omega^{\frac{p}{2}}_{uv}\left((f(v)-f(u))^{\pm}\right)^p\right)^{\frac{1}{p}}.$$

Similarly, for $p = \infty$, we define ∞-total variations as:

$$\mathrm{TV}_{\omega,\infty}(f) = \mathscr{I}\left(\left\|\nabla_{\omega}f(\cdot)\right\|_{\infty}\right) = \sum_{u \in V}\left(\max_{v \in V}\sqrt{\omega_{uv}}|f(v)-f(u)|\right)$$

$$\mathrm{TV}^{\pm}_{\omega,\infty}(f) = \mathscr{I}\left(\left\|\nabla^{\pm}_{\omega}f(\cdot)\right\|_{\infty}\right) = \sum_{u \in V}\left(\max_{v \in V}\sqrt{\omega_{uv}}(f(v)-f(u))^{\pm}\right).$$

In the local setting on the continuum, it is very well-known that the perimeter is linked to the total variation via the celebrated co-area formula. Similar results have been shown in [19, 40] on finite graphs. For the reader's convenience, we recall this result and its extension to the upwind and downwind p-total variations, for $p \in \{1, \infty\}$.

Proposition 4.1. *Let $G = (V, E, \omega)$ and $f : V \to \mathbb{R}$. Then*

$$\mathrm{TV}^{\pm}_{\omega,1}(f) = \int_{-\infty}^{+\infty}\mathrm{Per}^{\pm}_{\omega,1}(\{f > t\})dt, \tag{4.1}$$

$$\mathrm{TV}_{\omega,1}(f) = \int_{-\infty}^{+\infty}\mathrm{Per}_{\omega,1}(\{f > t\})dt. \tag{4.2}$$

PROOF :   For (4.2), see [40] and use Definition 3.2. For (4.1), combine (4.2), $\mathrm{TV}^{\pm}_{\omega,1}(f) = \frac{1}{2}\mathrm{TV}_{\omega,1}(f)$ and $\mathrm{Per}^{\pm}_{\omega,1}(\mathcal{A}) = \frac{1}{2}\mathrm{Per}_{\omega,1}(\mathcal{A})$ for any $\mathcal{A} \subset V$. $\qquad\square$

For $p = \infty$, the co-area formula holds for unweighted graphs, as the following proposition shows. To avoid any confusion, we will replace ω by $\{0, 1\}$ in the statement to stress the fact that the considered graph is unweighted.

Proposition 4.2. *Let $G = (V, E, \{0, 1\})$. For any function $f : V \to \mathbb{R}$, we have:*

$$\mathrm{TV}^{\pm}_{\{0,1\},\infty}(f) = \int_{-\infty}^{+\infty}\mathrm{TV}^{\pm}_{\{0,1\},\infty}(\chi_{\{f>t\}})dt,$$

$$\mathrm{TV}_{\{0,1\},\infty}(f) = \int_{-\infty}^{+\infty}\mathrm{TV}_{\{0,1\},\infty}(\chi_{\{f>t\}})dt.$$

PROOF :   Let $u \in V$ and let $v_u \in \mathcal{N}(u)$ such that $\left\|\nabla^{\pm}_{\{0,1\}}f(u)\right\|_{\infty} = (f(v_u) - f(u))^{\pm}$. It is easy to check that $\left\|\nabla^{\pm}_{\{0,1\}}\chi_{\{f>t\}}(u)\right\|_{\infty} = \left(\chi_{\{f>t\}}(v_u) - \chi_{\{f>t\}}(u)\right)^{\pm}$ for all $t \in \mathbb{R}$. It then follows that

$$\|\nabla^{\pm}_{\{0,1\}}f(u)\|_{\infty} = (f(v_u) - f(u))^{\pm}$$
$$= \int_{-\infty}^{+\infty}\left(\chi_{\{f>t\}}(v_u) - \chi_{\{f>t\}}(u)\right)^{\pm}dt$$

9

$$= \int_{-\infty}^{+\infty} \|\nabla_{\{0,1\}}^{\pm} \chi_{\{f>t\}}(u)\|_{\infty} dt$$

Hence,

$$\mathrm{TV}_{\{0,1\},\infty}^{\pm}(f) = \int_{-\infty}^{+\infty} \mathscr{I}\left(\left\|\nabla_{\{0,1\}}^{\pm} \chi_{\{f>t\}}(\cdot)\right\|_{\infty}\right) dt = \int_{-\infty}^{+\infty} \mathrm{Per}_{\{0,1\},\infty}^{\pm}(\{f>t\})dt,$$

where we invoked Definition 3.2 in the last equality. The second claim follows from the first ad the fat that $\mathrm{TV}_{\{0,1\},\infty}(f) = \mathrm{TV}_{\{0,1\},\infty}^{+}(f) + \mathrm{TV}_{\{0,1\},\infty}^{-}(f)$ and $\mathrm{Per}_{\{0,1\},\infty}(\mathcal{A}) = \mathrm{Per}_{\{0,1\},\infty}^{+}(\mathcal{A}) + \mathrm{Per}_{\{0,1\},\infty}^{-}(\mathcal{A})$ for any $\mathcal{A} \subset V$. $\qquad\square$

Remark 4.1. *For $p = \infty$, the co-area formula does not hold for general weighted graphs. Here is a counterexample. Let $G = (V, E, \omega)$ where $V = \{1, 2, 3\}$ and the weight function is given by*

$$\sqrt{\omega_{ij}} = \begin{cases} 1, & \text{if } (i,j) = (1,2), \\ 1/4, & \text{if } (i,j) = (1,3), \\ 1/3, & \text{if } (i,j) = (2,3). \end{cases}$$

Consider the following function defined on V as $f(1) = 0$, $f(2) = 1$ and $f(3) = 4$. By simple computations one gets that

$$\mathrm{TV}_{\omega,\infty}^{\pm}(f) = 2 < \frac{11}{4} = \int_{-\infty}^{+\infty} \mathrm{TV}_{\omega,\infty}^{\pm}(\chi_{\{f>t\}})dt,$$

$$\mathrm{TV}_{\omega,\infty}(f) = 3 < 5 = \int_{-\infty}^{+\infty} \mathrm{TV}_{\omega,\infty}(\chi_{\{f>t\}})dt.$$

We close this subsection with an application of the co-area formulas to an equivalent result on functional inequalities. For this, let $\mathcal{G}$ be a non-empty set of pairs (g_1, g_2) of functions in $\mathcal{H}(V)$, an let $\mathscr{L}$ be a functional generated by $\mathcal{G}$ as follows:

$$\mathscr{L} : f \in \mathcal{H}(V) \mapsto \sup_{(g_1,g_2) \in \mathcal{G}} \mathscr{I}(f^+ g_1 + f^- g_2). \tag{4.3}$$

We say that the functional $\mathscr{L}$ admits a quasi-linear representation. As noted in [39], many functionals have this representation, for example:

$$\mathscr{L}(f) = \left(\mathscr{I}\left(|f|^p\right)\right)^{1/p}, \text{ for } 1 \le p \le \infty,$$

$$\mathscr{L}(f) = \left(\mathscr{I}\left(|f - \mathscr{I}(f)|^p\right)\right)^{1/p}, \text{ for } 1 \le p \le \infty,$$

$$\mathscr{L}(f) = \inf_{a \in \mathbb{R}} \left(\mathscr{I}\left(|f - a|^p\right)\right)^{1/p} \text{ for } 1 \le p \le \infty.$$

We have the following equivalence.

Proposition 4.3. *Let $\lambda > 0$, and suppose that either $p = 1$ or $p = \infty$ and the graph is unweighted. Then the following are statements are equivalent:*

(i) $\mathscr{L}(f) \leq \lambda \mathrm{TV}_{\omega,p}^{\pm}(f)$ *for all* $f \in \mathcal{H}(V)$.

(ii) $\mathscr{L}(\chi_{\mathcal{A}}) \leq \lambda \mathrm{TV}_{\omega,p}^{\pm}(\chi_{\mathcal{A}})$ *and* $\mathscr{L}(-\chi_{\mathcal{A}}) \leq \lambda \mathrm{TV}_{\omega,p}^{\pm}(-\chi_{\mathcal{A}})$, *for all* $\mathcal{A} \subset V$.

PROOF : The implication (i) $\Longrightarrow$ (ii) is straightforward: it is enough to apply (i) to $f = \chi_A$ and $f = -\chi_{\mathcal{A}}$.

Conversely, suppose that (ii) and let $g_1, g_2 \in \mathcal{G}$. It is not difficult to see that

$$\mathrm{TV}_{\omega,p}^{\pm}(\chi_{\mathcal{A}}) = \mathscr{I}(\left\|\nabla_{\omega}^{\pm}\chi_{\mathcal{A}}(\cdot)\right\|_p) = \mathscr{I}(\left\|\nabla_{\omega}^{\pm}(-\chi_{\mathcal{A}^c})(\cdot)\right\|_p) = \mathrm{TV}_{\omega,p}^{\pm}(-\chi_{\mathcal{A}^c}),$$

for all $\mathcal{A} \subset V$. Therefore, the co-area formula in Proposition 4.1 for $p = 1$ (resp. Proposition 4.2 for $p = \infty$ and the graph is unweighted) implies

$$\begin{aligned}
\mathrm{TV}_{\omega,p}^{\pm}(f) &= \int_0^{+\infty} \mathscr{I}(\left\|\nabla_{\omega}^{\pm}\chi_{\{f>t\}}(\cdot)\right\|_p)dt + \int_{-\infty}^0 \mathscr{I}(\left\|\nabla_{\omega}^{\pm}\chi_{\{f>t\}}(\cdot)\right\|_p)dt \\
&= \int_0^{+\infty} \mathscr{I}(\left\|\nabla_{\omega}^{\pm}\chi_{\{f>t\}}(\cdot)\right\|_p)dt + \int_{-\infty}^0 \mathscr{I}(\left\|\nabla_{\omega}^{\pm}(-\chi_{\{f\leq t\}})(\cdot)\right\|_p)dt \\
&\geq \lambda^{-1} \int_0^{\infty} \mathscr{L}(\chi_{\{f>t\}})dt + \lambda^{-1} \int_{-\infty}^0 \mathscr{L}(-\chi_{\{f\leq t\}})dt \\
&\geq \lambda^{-1} \int_0^{\infty} \mathscr{I}\left(\chi_{\{f>t\}}g_1\right)dt + \lambda^{-1} \int_{-\infty}^0 \mathscr{I}\left(\chi_{\{f\leq t\}}g_2\right)dt \\
&= \lambda^{-1} \left(\mathscr{I}\left(f^+g_1 + f^-g_2\right)\right).
\end{aligned}$$

We get the desired inequality by taking the supremum over all function $g_1, g_2 \in \mathcal{G}$. $\square$

5 Mean curvature on graphs

We here introduce a class of mean curvatures on graphs based on the definition of the nonlocal perimeters on graphs defined above. As in the nonlocal continuum case [13], we adopt a variational formulation and define the mean curvature as the first variation of the perimeter. We recall that $\delta(u)$ is the degree of a vertex $u \in V$.

Definition 5.1. *Let* $G = (V, E, \omega)$, $\mathcal{A} \subset V$, *and* $u_0 \in V$. *We define the upwind and downwind mean curvatures of* $\mathcal{A}$ *at* u_0 *as*

$$\kappa_{\omega,1}^+(u_0, \mathcal{A}) \stackrel{\mathrm{def}}{=} \frac{\mathrm{Per}_{\omega,1}^+(\mathcal{A} \cup \{u_0\}) - \mathrm{Per}_{\omega,1}^+(\mathcal{A})}{\delta(u_0)},$$

$$\kappa_{\omega,1}^-(u_0, \mathcal{A}) \stackrel{\mathrm{def}}{=} \frac{\mathrm{Per}_{\omega,1}^-(\mathcal{A}) - \mathrm{Per}_{\omega,1}^-(\mathcal{A} \setminus \{u_0\})}{\delta(u_0)}.$$

The mean curvature of $\mathcal{A}$ *ate* $u_0 \in V$ *is defined as*

$$\kappa_{\omega,1}(u_0, \mathcal{A}) \stackrel{\mathrm{def}}{=} \begin{cases} \kappa_{\omega,1}^+(u_0, \mathcal{A}), & \text{if } u_0 \in \mathcal{A}^c, \\ \kappa_{\omega,1}^-(u_0, \mathcal{A}), & \text{if } u_0 \in \mathcal{A}. \end{cases}$$

11

From Definition 3.2, it is straightforward to show that

$$\mathrm{Per}^+_{\omega,1}(\mathcal{A} \cup \{u_0\}) - \mathrm{Per}^+_{\omega,1}(\mathcal{A}) = \begin{cases} \sum_{v \in \mathcal{A}^c} \sqrt{\omega_{u_0 v}} - \sum_{v \in \mathcal{A}} \sqrt{\omega_{u_0 v}} & \text{if } u_0 \in \mathcal{A}^c, \\ 0 & \text{if } u_0 \in \mathcal{A}, \end{cases}$$

and

$$\mathrm{Per}^-_{\omega,1}(\mathcal{A}) - \mathrm{Per}^-_{\omega,1}(\mathcal{A} \setminus \{u_0\}) = \begin{cases} \sum_{v \in \mathcal{A}^c} \sqrt{\omega_{u_0 v}} - \sum_{v \in \mathcal{A}} \sqrt{\omega_{u_0 v}} & \text{if } u_0 \in \mathcal{A}, \\ 0 & \text{if } u_0 \in \mathcal{A}^c. \end{cases}$$

We have then proved the following explicit formula of the mean curvature on a graph.

Proposition 5.1. *Let $G = (V, E, \omega)$. For all $\mathcal{A} \subset V$ and all $u_0 \in V$, we have:*

$$
\begin{aligned}
\kappa_{\omega,1}(u_0, \mathcal{A}) &= \frac{\sum_{v \in \mathcal{A}^c} \sqrt{\omega_{u_0 v}} - \sum_{v \in \mathcal{A}} \sqrt{\omega_{u_0 v}}}{\delta(u_0)} \\
&= -\frac{\sum_{v \in V} \sqrt{\omega_{u_0 v}} (\chi_{\mathcal{A}}(v) - \chi_{\mathcal{A}^c}(v))}{\delta(u_0)}.
\end{aligned}
\tag{5.1}
$$

Before proceeding, a few remarks are in order.

Remark 5.1. *(i) One can see that our definition implies a curvature which is bounded and belongs to $[-1, 1]$. The reason lies in the normalization by the degree of the associated vertex.*

(ii) In view of (5.1), we can extend this definition of mean curvature to any function f on graphs through its level sets. Indeed, let $f : V \to \mathbb{R}$ and $u_0 \in V$. The mean curvature $\kappa_{\omega,1}$ (we keep the same notion) of f at u_0 on a graph $G = (V, E, \omega)$ is defined as

$$
\begin{aligned}
\kappa_{\omega,1}(u_0, f) &\overset{\text{def}}{=} \kappa_{\omega,1}(u, \{f \geq f(u_0)\}) \\
&= -\frac{\sum_{v \in \{f \geq f(u_0)\}} \sqrt{\omega_{u_0 v}} - \sum_{v \in \{f < f(u_0)\}} \sqrt{\omega_{u_0 v}}}{\delta(u_0)} \\
&= -\frac{\sum_{v \in V} \sqrt{\omega_{u_0 v}} \, \mathrm{sign}(f(v) - f(u_0))}{\delta(u_0)},
\end{aligned}
\tag{5.2}
$$

where

$$\mathrm{sign}(r) = \begin{cases} 1, & \text{if } r \geq 0, \\ -1, & \text{if } r < 0. \end{cases}$$

(iii) Formula (5.1) can also be interpreted as a graph version of the nonlocal J-mean curvature introduced in [28, Definition 3.2], which is given, for a measurable set $\mathcal{E} \subset \mathbb{R}^n$ and $n \geq 2$ by

$$H^J_{\partial\mathcal{E}}(\boldsymbol{x}) \overset{\text{def}}{=} -\int_{\mathbb{R}^n} J(\boldsymbol{x} - \boldsymbol{y})(\chi_{\mathcal{E}}(\boldsymbol{y}) - \chi_{\mathcal{E}^c}(\boldsymbol{x}))d\boldsymbol{y}, \qquad x \in \mathbb{R}^n,$$

where J is a nonnegative radially symmetric measurable function in $L^1(\mathbb{R}^n)$. For $\varepsilon > 0$, let $J_\varepsilon(\boldsymbol{x}) = \varepsilon^{-n} J(\boldsymbol{x}/\varepsilon)$ be the rescaled kernel, and set $C_J = 2 \left(\int_{\mathbb{R}^n} J(\boldsymbol{x})|\boldsymbol{x}_n|d\boldsymbol{x} \right)^{-1}$. It was shown in [28, Theorem 3.7] that for $\mathcal{E}$ with smooth enough boundary $\partial\mathcal{E}$, we have

$$\lim_{\varepsilon \searrow 0} \frac{C_J}{\varepsilon} H^{J_\varepsilon}_{\partial\mathcal{E}}(\boldsymbol{x}) = (n-1)\kappa(\boldsymbol{x}),$$

for every $\boldsymbol{x} \in \partial\mathcal{E}$, where $\kappa(\boldsymbol{x})$ is the (local) mean curvature of ∂E at $\boldsymbol{x}$. defined by

$$\kappa(\boldsymbol{x}) = -\mathrm{div}(n_{\boldsymbol{x}}), \tag{5.3}$$

where $n_{\boldsymbol{x}}$, $\boldsymbol{x} \in \partial E$, is the unit normal vector field.

(iv) *Inspired by the local formula* (5.3) *on the continuum, let us discuss a discrete analogue of it on graphs. This idea was first proposed in [40]. Let $G = (V, E, \omega)$ be a weighted graph. For a nonempty set $\mathcal{A} \subset V$, let*

$$\kappa^{\mathrm{loc}}_{\omega,1}(u, \mathcal{A}) = \mathbf{div}_{\omega}(n_{\mathcal{A}})(u) = \begin{cases} \sum_{v \in \mathcal{A}^c} \sqrt{\omega_{uv}}, & \text{if } u \in \mathcal{A}, \\ -\sum_{v \in \mathcal{A}} \sqrt{\omega_{uv}}, & \text{if } u \in \mathcal{A}^c, \end{cases} \tag{5.4}$$

where $n_{\mathcal{A}}$ is the discrete normal vector defined as

$$n_{\mathcal{A}}(u, v) = \begin{cases} 1 & \text{if } u \sim v \text{ and } (u, v) \in \mathcal{A} \times \mathcal{A}^c, \\ -1 & \text{if } u \sim v \text{ and } (u, v) \in \mathcal{A}^c \times \mathcal{A}, \\ 0 & \text{otherwise.} \end{cases}$$

Observe in passing that the formula given in [40] is different from (5.4). *The difference essentially lies in the definition of the divergence operator they consider. Observe also that the sign of the mean curvature given by* (5.4), *depends only on the side that contains the vertex u and not on the weight function. This is in stark contrast with the mean curvature introduced in Definition 5.1 (see also Proposition 5.1). This has impact in applications and it would be worth getting deeper insight into these differences in a future work. In the rest of this work, and especially in our numerical experiments, we will stick with Definition 5.1.*

(v) *A natural question that comes to mind is whether the mean curvature on graphs in Proposition 5.1 can be given a limit in an appropriate sense as the number of vertices grows to infinity. In particular, can one prove rigorously that it has a continuum local limit as N grows and by properly rescaling the weight function ω with a vanishing width, and whether this limit relates to the (local) mean curvature* (5.3). *In fact, the same questions arise also on other geometrical quantities including the perimeter. These are important questions that are beyond the scope of this paper and deserve much deeper investigation that we leave to a future work.*

6   Level set formulation of mean curvature flows on graphs

Equipped with our graph versions of differential operators and mean curvature, we are now ready to adapt to graphs a large class of PDEs involving the mean curvature flow or its variants. In this section, we consider two general models used extensively to solve several tasks in image processing and computer vision:

1. The level set method for power mean curvature flow which finds applications in image denoising, enhancement or simplification;

2. The level set method for active contours with application to image segmentation and object detection.

The transposition of these models on graphs will naturally lead to partial difference equations (coined PdE's for short) with coefficients that depend on the data and the graph weight function.

6.1 The continuum domain case

The level set approach was first proposed by Osher and Sethian [34] to model evolving fronts with curvature; see also the monographs [31, 10]. The idea is to represent the evolving front as a level set of a function $\phi(\boldsymbol{x}, t)$ for $\boldsymbol{x} \in \Omega \subset \mathbb{R}^n$ and t is the time. The initial front Γ_0 is given by $\Gamma_0 = \{\boldsymbol{x} \in \Omega : \phi(\boldsymbol{x}, 0) = \phi_0(\boldsymbol{x}) = 0\}$, where ϕ_0 is a smooth function on Ω, and the evolving front at any time $t > 0$ is given by $\Gamma_t = \{\boldsymbol{x} \in \Omega : \phi(\boldsymbol{x}, t) = 0\}$. The evolving front is governed by the following equation:

$$\begin{cases} \frac{\partial \phi}{\partial t}(\boldsymbol{x}, t) = c(\boldsymbol{x}, \phi, t) \big\| \nabla \phi(\boldsymbol{x}, t) \big\|_2, & (\boldsymbol{x}, t) \in \Omega \times]0, T] \\ \phi(\boldsymbol{x}, 0) = \phi_0(\boldsymbol{x}), & \boldsymbol{x} \in \Omega, \end{cases} \tag{6.1}$$

where $c(\boldsymbol{x}, \phi, t)$ is a normal velocity governing the motion.

6.1.1 Level set power mean curvature flow

Making the choice

$$c(\boldsymbol{x}, \phi, t) = \big| \kappa(\boldsymbol{x}, t) \big|^{\alpha - 1} \kappa(\boldsymbol{x}, t), \tag{6.2}$$

where $\alpha \in [0, 1]$ and κ is the usual mean curvature, one gets the level set power mean curvature equation, [33]. In particular, for $\alpha = 1$, (6.1) corresponds to the mean curvature flow which finds important applications in image processing [34], while the case where $\alpha \to 0$, one gets the so called conditional erosion/dilatation based on the sign of the mean curvature used in mathematical morphology. A variant for positive/negative curvature flows are used in [27] for image enhancement in addition to noise removal.

6.1.2 Level set active contours

This corresponds to the situation in (6.1) where ϕ_0 is an implicit representation of a front (surface) and the following choice of velocity

$$c(\boldsymbol{x}, \phi, t) = \operatorname{div} \left(\frac{\nabla \phi(\boldsymbol{x}, t)}{\big\| \nabla \phi(\boldsymbol{x}, t) \big\|_2} \right) + F(I, \phi(\boldsymbol{x}, t)), \tag{6.3}$$

where $I : \Omega \to \mathbb{R}$ is the image to be segmented and F is a halting function of the active contour model. The level set formulation of active contours is one of the most popular variational models in image segmentation. Its success is due to strong mathematical properties, efficient numerical schemes and ability to handle topological changes naturally.

The Chan-Vese model for active contours [15, 41] offers a flexible method which localizes objects whose boundaries are not well-detected by the gradient. This model corresponds to a special case of (6.3) where the halting function takes the form

$$F(I, \phi(\boldsymbol{x}, t)) = -\lambda_1 (I - c_1)^2 + \lambda_2 (I - c_2)^2 \tag{6.4}$$

14

where $\lambda_1, \lambda_2 > 0$ are the fidelity parameters, and c_1 (resp. c_2) is the average of I on the superlevel set $\{\boldsymbol{x} \in \Omega : \phi(\boldsymbol{x}, t) \geq 0\}$ (resp. on the sublevel set $\{\boldsymbol{x} \in \Omega : \phi(\boldsymbol{x}, t) \leq 0\}$).

6.2 Level set power mean curvature flow on graphs

Let us now turn to translating on graphs the PDE (6.1) with the velocity (6.2). Let $G = (V, E, \omega)$ be a weighted graph. Our formulation of the level set power mean curvature equation on G is

$$\begin{cases} \frac{\partial \phi}{\partial t}(u, t) &= \left(\left| \kappa_{\omega,1}(u, \phi(\cdot, t)) \right|^{\alpha-1} \kappa_{\omega,1}(u, \phi(\cdot, t)) \right)^+ \left\| \nabla_\omega^+ \phi(u, t) \right\|_p, \\ &\quad - \left(\left| \kappa_{\omega,1}(u, \phi(\cdot, t)) \right|^{\alpha-1} \kappa_{\omega,1}(u, \phi(\cdot, t)) \right)^- \left\| \nabla_\omega^- \phi(u, t) \right\|_p, \ (u, t) \in V \times]0, T], \\ \phi(u, 0) &= \phi_0(u), \quad u \in V \end{cases} \quad (6.5)$$

where $\phi_0 \in \mathcal{H}(V)$, $\alpha \in [0, 1]$, $p \in [1, +\infty]$, and we recall from (5.2) that

$$\kappa_{\omega,1}(u, \phi(\cdot, t)) = \kappa_{\omega,1}\left(u, \{\phi(\cdot, t) \geq \phi(u, t)\}\right).$$

To implement numerically (6.5), we use a simple forward/explicit Euler discretization scheme in time. Let $0 < t_1 < t_2 < \cdots < t_\ell = T$ be an equispaced partition of $[0, T]$, $T > 0$, i.e., $t_i = i\Delta t$ for $i \in [\ell]$ with $\Delta t = \frac{T}{\ell}$. Denote $\phi^i(u) = \phi(u, i\Delta t)$. Starting at $\phi^0 = \phi_0$, we then propose the iterative scheme

$$\phi^{i+1}(u) = \phi^i(u) + \Delta t \Bigg(\left(\left| \kappa_{\omega,1}(u, \phi^i(u)) \right|^{\alpha-1} \kappa_{\omega,1}(u, \phi^i(u)) \right)^+ \left\| \nabla_\omega^+ \phi^i(u) \right\|_p$$

$$- \left(\left| \kappa_{\omega,1}(u, \phi^i(u)) \right|^{\alpha-1} \kappa_{\omega,1}(u, \phi^i(u)) \right)^- \left\| \nabla_\omega^- \phi^i(u) \right\|_p \Bigg). \quad (6.6)$$

Note that for $p = \infty$, we recover as a special case the scheme considered in [19, Section 3.3].

Another case of interest is when when $\alpha = 0$ and $p = \infty$, in which case it is straightforward to see that (6.6) reads

$$\phi^{i+1}(u) = \begin{cases} \phi^i(u) + \Delta t \left\| \nabla_\omega^+ \phi^i(u) \right\|_\infty, & \text{if } \kappa_\omega(\phi^i(u)) \geq 0, \\ \phi^i(u) - \Delta t \left\| \nabla_\omega^- \phi^i(u) \right\|_\infty, & \text{if } \kappa_\omega(\phi^i(u)) < 0. \end{cases} \quad (6.7)$$

For the choice $\Delta t = 1$, the update (6.7) has a nice interpretation in mathematical morphology: it is a conditional erosion/dilatation on graphs based on the sign of the mean curvature.

6.3 Level set active contour on graphs

For $G = (V, E, \omega)$ a weighted graph, a front evolving on G is a subset $\mathcal{A}_0 \subset V$, and is implicitly represented by a level set function $\phi_0 = \chi_{\mathcal{A}_0} - \chi_{\mathcal{A}_0^c}$. In other words, ϕ_0 takes the value 1 on $\mathcal{A}_0$ and -1 on its complement. Mimicking the PDE (6.1) on the continuum with the velocity (6.3), the front propagation equation on G is given by

$$\begin{cases} \frac{\partial \phi}{\partial t}(u, t) = c(u, \phi, t) \left\| \nabla_\omega \phi(u, t) \right\|_p, & (u, t) \in V \times]0, T] \\ \phi(u, 0) = \phi_0(u), & u \in V, \end{cases} \quad (6.8)$$

15

where $c(u, \phi, t)$ is given by

$$c(u, \phi, t) = \kappa_{\omega,1}(u, \phi(\cdot, t)) + F(I, \phi(u, t)), \tag{6.9}$$

with halting function F and $I : V \to \mathbb{R}$ is the function on V to be segmented. Typically we will take in our numerical experiments F as in (6.4), where now c_1 (resp. c_2) is the average of I on $\{u \in V : \phi(u, t) \geq 0\}$ (resp. on $\{u \in V : \phi(u, t) \leq 0\}$).

Yet another form can be proposed based on discrete dilation and erosion on graphs. Indeed, the front propagation can be expressed as a morphological process with the following sum of dilation and erosion

$$\begin{cases} \frac{\partial \phi}{\partial t}(u, t) & = (c(u, \phi, t))^+ \cdot \left\| \nabla_\omega^+ \phi(u, t) \right\|_p \\ & \quad - (c(u, \phi, t))^- \cdot \left\| \nabla_\omega^- \phi(u, t) \right\|_p, \quad (u, t) \in V \times]0, T] \\ \phi(u, 0) & = \phi_0(u), \quad u \in V. \end{cases} \tag{6.10}$$

As before, Euler explicit/forward discretization in time then leads to the iterative scheme

$$\phi^{i+1}(u) = \phi^i(u) + \Delta t \left(c(u, \phi^i, t_i)^+ \left\| \nabla_\omega^+ \phi^i(u) \right\|_p - c(u, \phi^i, t_i)^- \left\| \nabla_\omega^- \phi^i(u) \right\|_p \right) \tag{6.11}$$

$$= \begin{cases} \phi^i(u) + \Delta t \, c(u, \phi^i, t_i) \left\| \nabla_\omega^+ \phi^i(u) \right\|_p, & \text{if } c(u, \phi^i, t_i) \geq 0, \\ \phi^i(u) + \Delta t \, c(u, \phi^i, t_i) \left\| \nabla_\omega^- \phi^i(u) \right\|_p, & \text{if } c(u, \phi^i, t_i) < 0. \end{cases} \tag{6.12}$$

The last form of the update highlights the fact that one only has to compute one morphological gradient at each iteration, for a given vertex. Moreover, one can remark that at initialization, given the form of ϕ_0 above, both two gradients are zero everywhere, except for vertices which lies in the inner and outer boundaries of $\mathcal{A}_0$. Then, the set of vertices to be updated at each iteration can be restricted to two inner and outer narrow bands, initialized respectively with $\partial^- \mathcal{A}_0$ and $\partial^+ \mathcal{A}_0$ and updated over time with neighbours of vertices already in them. The narrow bands growth follows the front evolution, and to avoid that they become too large, the narrow bands are reinitialized periodically. Clearly, for a given period $K \in \mathbb{N}$, the front is given by the set $\mathcal{A}_k = \{u \in V : \phi^i(u) > 0\}$ if $k = i/K \in \mathbb{N}$, and the associated level set function is reinitialized to $\phi^k(u) = \chi_{\mathcal{A}_k}(u) - \chi_{\mathcal{A}_k^c}(u)$. Then, the inner and outer narrow bands are respectively reinitialized as $\partial^- \mathcal{A}_k$ and $\partial^+ \mathcal{A}_k$.

Remark 6.1. *It is worth observing that from the general form* (6.10), *one can also obtain a graph version of the Eikonal equation which describes a morphological erosion process. Indeed, taking constant velocity $c(u, \phi, t) = 1$, zero initial data, and defining $\phi(u, t) = t - \varphi(u)$ for all $u \in V$,* (6.10) *reads*

$$\begin{cases} \left\| \nabla_\omega^- \varphi(u) \right\| = 1, & u \in V_0, \\ \varphi(u) = 0, & u \in V \setminus V_0, \end{cases} \tag{6.13}$$

where $V_0 \subset V$. Numerical schemes and algorithms to solve such equation have provided in [17]. This equation will be used in our numerical experiments on segmentation.

7 Numerical experiments

In this section, we describe our numerical experiments to illustrate the applicability and flexibility of our framework for data denoising and segmentation. This allows us to handle in the same framework both images, 3D point clouds ad other high dimensional data. Different graph structures and weight functions are also used to show the flexibility of our approach.

7.1 Weighted graph construction

Given N data points $\{x_i\}_{i \in [N]}$ on some space $\mathcal{X}$, there exist several popular methods to transform this dataset into a weighted graph structure. Each x_i is considered as a vertex $u_i \in V$ of a graph. The key now is to construct the adjacency structure of the graph, i.e., the set of edges E and weight function ω. This amounts to capturing the neighbourhood relationships between the data points by typically exploiting some similarity between features computed from the points $\{x_i\}_{i \in [N]}$. This is clearly application-dependent and we will describe some concrete examples shortly.

In the particular case of images, graph construction methods based on spatial neighbourhoods are particularly well-adapted to capture the geometry of the space. The spatial neighbourhood can also be augmented by similarity of feature values defined on the pixels. Typical types of graphs used in practice are:

- *Grid graphs*: these are the most natural ones to describe an image with a graph. The points $\{x_i\}_{i \in [N]}$ are then the coordinates of the image pixels lying on a cartesian grid. Each pixel/point is connected by an edge to its spatial adjacent neighbours. Classical grid graphs are 4-adjacency grid graphs and 8-adjacency grid graphs. Larger neighbourhoods can be used to obtain nonlocal grid graphs.

- *Region adjacency graphs* (RAGs): the vertices of these graphs correspond to regions in an image and edges represent region spatial adjacency relationships.

- *k-nearest neighbour graphs* (*k*-NNGs): in these graphs, $(\mathcal{X}, d)$ is a metric space, and each vertex $u_i \in V$, or equivalently each data point $x_i \in \mathcal{X}$, is connected to its k-nearest neighbours according to the distance d, and possibly a distance between features computed at $\{x_i\}_{i \in [N]}$. Such construction implies building a directed graph as the neighbourhood relationship is not necessarily symmetric. Nevertheless, an undirected graph can be obtained by adding an edge (u, v) whenever u is among the k-nearest neighbours of v or v is among the k-nearest neighbours of u.

- *k-extended RAGs* (*k*-ERAGs): these are RAGs augmented by a k-NNG. Each vertex corresponds to a region which is connected to its spatially adjacent regions and to its k most similar regions in the metric d.

The weight function is computed as a function of a similarity measure $s : E \rightarrow \mathbb{R}^+$ as follows

$$\omega_{uv} = \begin{cases} s(u, v), & \text{if } (u, v) \in E, \\ 0, & \text{otherwise.} \end{cases} \tag{7.1}$$

Examples for common similarity functions are the following.

- $s_0(u, v) = 1$: this corresponds to a simple unweighted graph.

- $s_1(u, v) = \exp(-d(u, v)^2/\sigma^2)$, where $V = \{x_i\}_{i \in [N]}$, $(\mathcal{X}, d)$ is a metric space, and $\sigma > 0$ is a scale parameter that represents the size of the neighbourhood.

- Patch-based methods: let $p : V = \{x_i\}_{i \in [N]} \subset \mathcal{X} \in \mathbb{R}^m$ be a patch extractor, i.e., a mapping acting on the data points and returning an m-dimensional real feature vector. In many applications we have in mind, p extracts the spatial coordinate, the values of a function defined on $\{x_i\}_{i \in [N]}$, etc. Let h be a metric on $\mathbb{R}^m$. In this context, a similarity function can be chosen as

$$s_2(u, v) = \exp(-h(p(u), p(v))^2/\sigma^2), \text{ with } \sigma > 0.$$

Observe that s_2 specializes to s_1 when p is the identity map.

7.2 Mean curvature flow

We start by illustrating the discrete mean curvature flow scheme (6.6) for denoising real image data, defined on a two-dimensional cartesian grid and then on a 3D point cloud.

Figure 1 depicts a comparison between the denoising results of a noisy image using (6.6) with $p = 2$ and two graph structures. The row with images (b-c-d) shows the results obtained with a 4-adjacency grid graph, which captures local interactions, and a weight function ω taken as in (7.1) with $s = s_0$. The row with images (e-f-g) shows the results obtained with a graph built as a k-NNG with a 16×16 spatial neighbourhood window and a weight function taken as in (7.1) with $s = s_2$, h the Euclidean distance and $\sigma = 20$. The feature space dimension m is the size of the patch: 5×5. Clearly, allowing long-range interaction thanks to the second graph structure better preserves the image details.

Figure 2 displays denoising results of a real color image using again (6.6) with $p = 2$ and two graph structures. For the 4-adjacency grid graph, we tested a weight function ω taken as in (7.1) with two choices of the similarity function: $s = s_0$ and $s = s_1$. The second graph is built using a k-NNG with a 11×11 spatial neighbourhood window and a weight function taken as in (7.1) with $s = s_2$, h the Euclidean distance and $\sigma = 20$. The feature space is $\mathbb{R}^{25 \times 3}$ corresponding to color images with patch size 5×5. These results show the effects of the similarity measure on the results. As in the previous experiment, the long-term interactions and patch-based weight functions give better results.

Te flexibility of our framework allows to handle with little effort functions on 3D point clouds. Figure 3 shows denoising results obtained in this setting. We used two graph structures, both built from the same 3D point clouds using a k-NNG, with $k = 8$ and s_0 as a similarity measure for the first one. For the second one, we took $k = 10$ and $s(u, v) = \exp(-\|\phi_0(u) - \phi_0(v)\|^2/10^2)$, where ϕ_0 is the initial datum taking values in the RGB cube.

7.3 Active contour model on graphs

7.3.1 Image segmentation using grid and k-NN graphs

We first illustrate the application to images of (6.11) with velocity (6.9), where F is set as in (6.4) (Chan-Vese model). Figure 4 and Figure 5 show the segmentation results with two different graph structures, respectively. Figure 4, we used a 4-adjacency grid graph where each
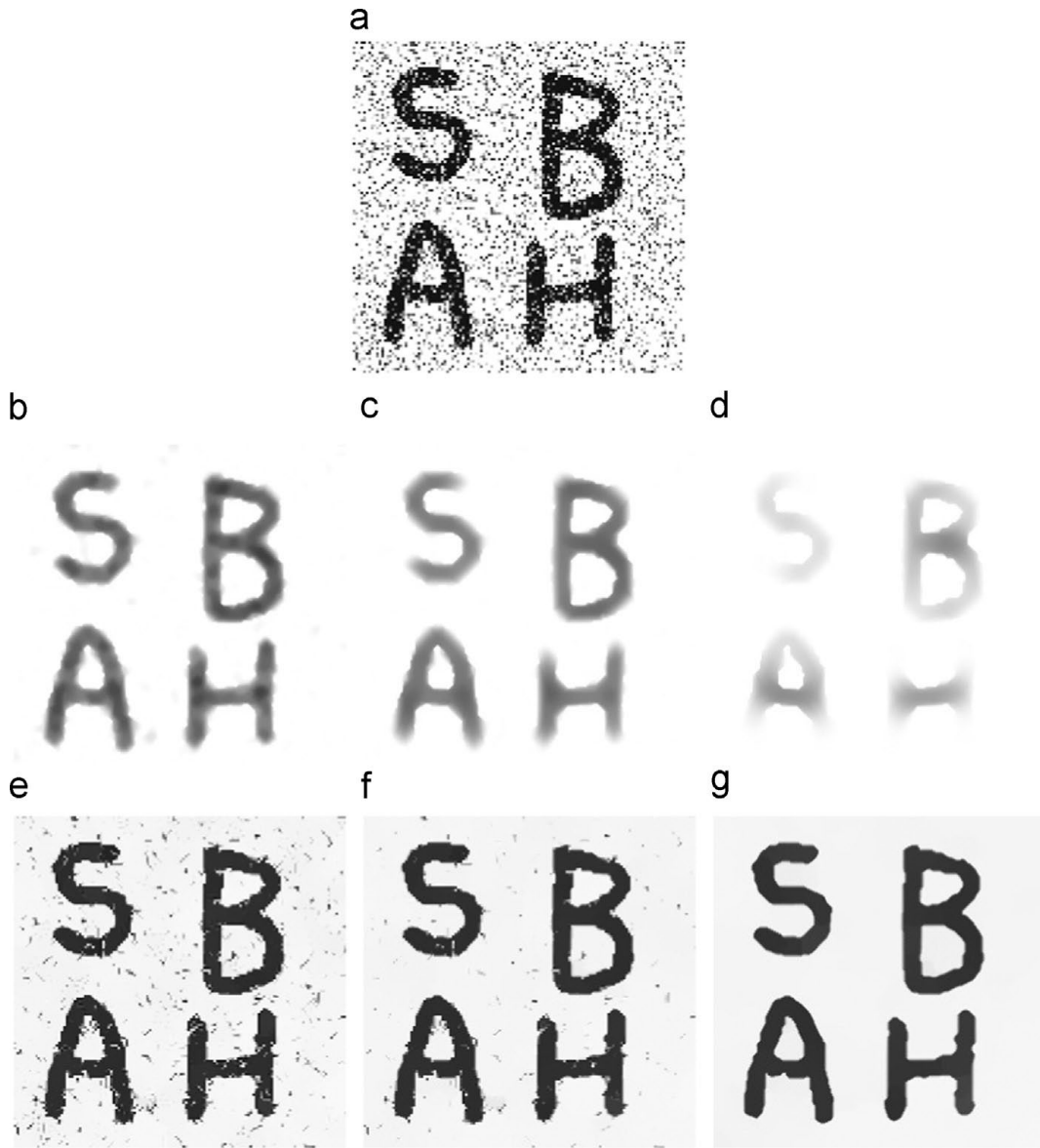
Figure 1: Gray scale image denoising. (a): observed image. (b,c,d): denoising results using mean curvature on a 4-adjacency grid graph after 5, 10, 20 iterations respectively. (e,f,g): denoising results using mean curvature on a k-NNG graph with patch-based weights after 5, 10, 20 iterations respectively.

pixel is characterized by its color feature vector. In Figure 5, we used a k-NNG with a 11×11 neighbourhood, and each pixel is characterized by a 5×5 patch of color feature vectors. In each case, the weight function is chosen as in the previous section. In Figure 4, we also tested the k-NNG though the results are not shown. Given that the image of Figure 4 does not contain textures, there was no significant difference between the segmentation results obtained by the two types of graphs. On the other hand, with the texture of the grass in the background of the image in Figure 5, the k-NNG with patch-based similarity leads to a better segmentation

(a) Original image   (b)

(c)   (d)
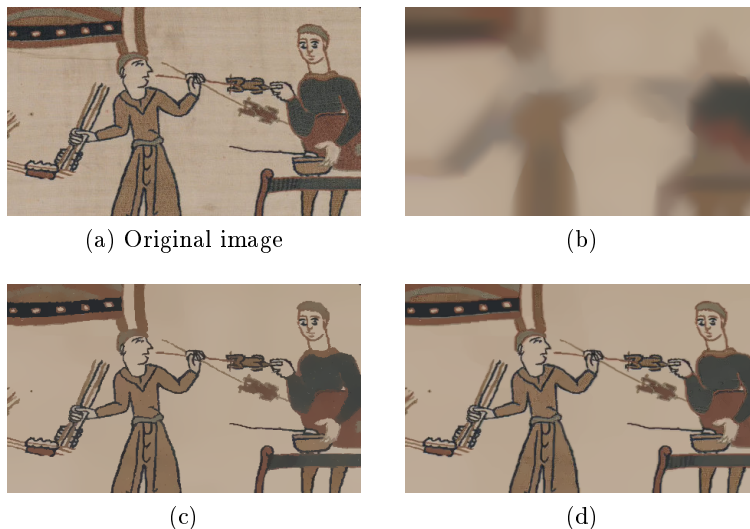
Figure 2: Color scale image denoising. (a): observed image. (b) and (c): denoising results using mean curvature on a 4-adjacency grid graph with respectively, s_0 and s_1 as similarity measures. (f): denoising result using mean curvature on a k-NNG graph with patch-based similarity measure s_2.

result. The bottomline is that k-NNG is a better choice and leads to better results thanks to its nonlocal aspect allowing to capture long range dependencies such as in textures.

7.3.2   Image segmentation using RAG

We here combine the graph-based versions of Eikonal equation (6.13) and active contours (6.11) for segmentation purposes. The active contour evolution (6.11) is performed on a RAG obtained from a superpixel decomposition of the image. Such decomposition is performed using a regular-grid of seeds, which are dilated on the image 4-adjacency-grid graph using the graph version of the Eikonal equation (6.13); see [18] for details. The resulting region map is then transformed in a second graph (the RAG) where each node is associated with a superpixel and edges represent the adjacency between superpixels. For the 4-adjacency-grid graph, the similarity function is computed from pixel colors, while it uses region mean intensity for the RAG. We then apply (6.13) on the RAG. Finally, the contour at convergence of the algorithm is transposed from the graph to the region map and then to the original image. Figure 6 depicts each step of the whole process.

7.3.3   Data clustering

In this experiment, we show that our level set active contour method can also be used for data clustering purposes, when data are represented as point clouds. To do so, we have selected a small part of the MNIST dataset [26]. This dataset is composed of handwritten digits, stored as images. The subset we choose is composed of 2 classes : 0's and 1's. For illustration we picked up 200 images of each class. We constructed a k-NN graph on this dataset, with $k = 5$. To compute the distance between two images, we used the two-sided tangent distance [25],
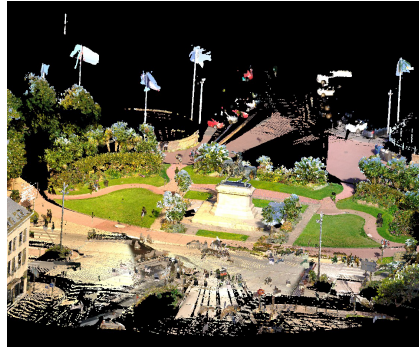
(a) Original image

(b)
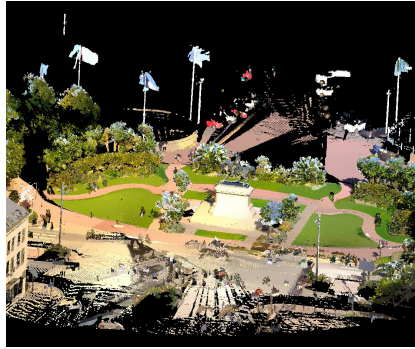
(c)

Figure 3: Colored point cloud denoising with mean curvature flow. (a): observed image. (b): denoising result using a k-NNG with $k = 8$ and ω with the similarity measure s_0. (c): denoising result using a k-NNG with $k = 10$ and ω with a feature-based similarity measure (see text for details).
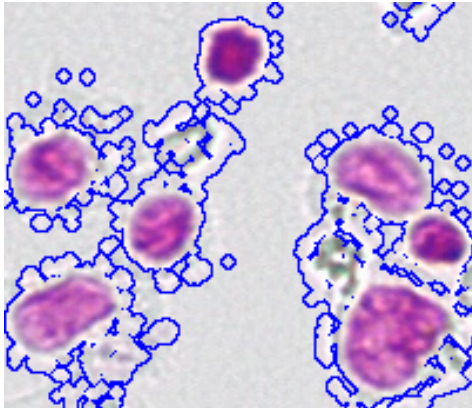
(a) Initial contour
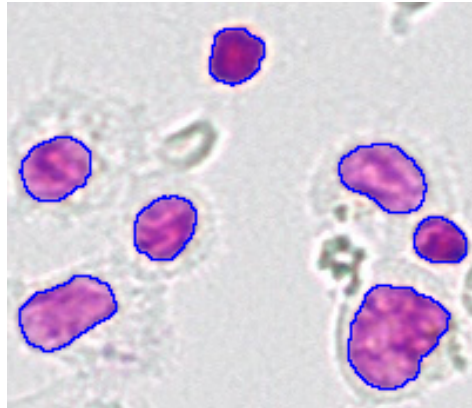
(b) Final contour

Figure 4: Segmentation using (6.11) with velocity (6.9) and Chan-Vese model. The graph used is a 4-adjacency grid graph and each pixel is characterized by its color feature vector.

(a) Initial contour   (b) Final contour
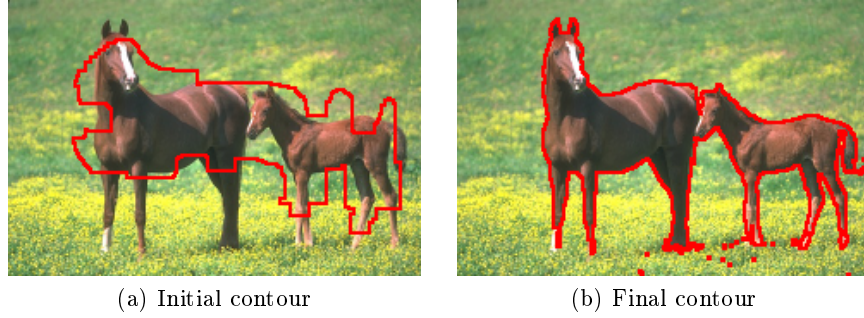
Figure 5: Segmentation using (6.11) with velocity (6.9) and Chan-Vese model. The graph is a k-NNG and each pixel is characterized by its color feature vector.
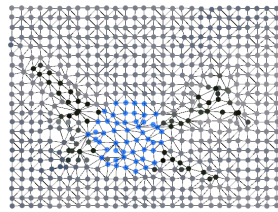
(a) RAG, front and bands   (b) Contour reported on image
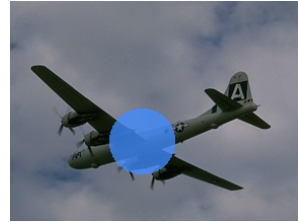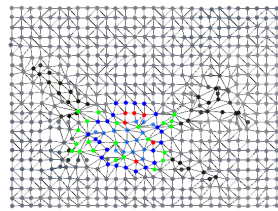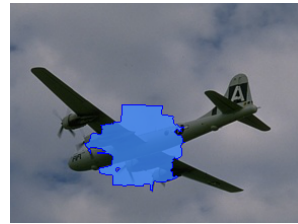
(c) After one iteration   (d) After one iterations
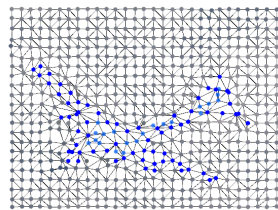
(e) After 82 iterations   (f) After 82 iterations

Figure 6: Illustration of active contours on a RAGG. The RAG is built from a superpixel decomposition of the initial image, where each region is connected to its adjacent regions. The weight and velocity functions are computed from the mean color inside regions. Left column shows the RAG, with the propagating front in blue and candidate bands in red (inner) and green (outer). Right column shows the initial image with the propagating front transposed from the RAG (using the boundaries of the superpixels).

an extension of the tangent distance used in [36], especially well suited for this dataset. The graph and several iterations of the scheme are shown in Figure 7. The scheme starts with an initial random partition.
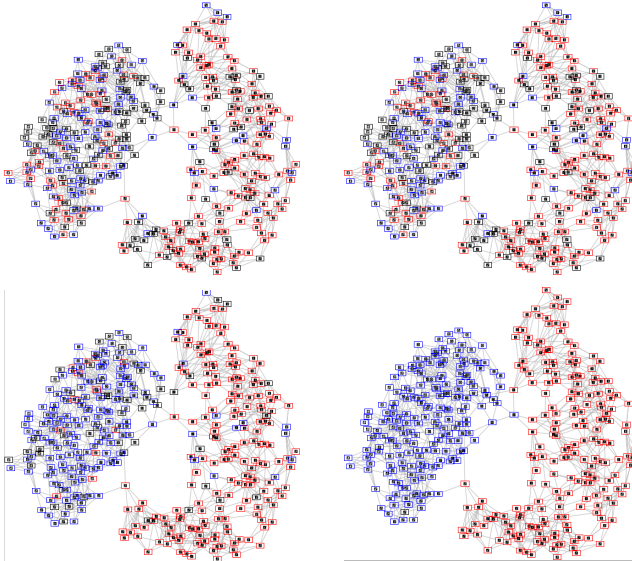
Figure 7: Application of the level set active contours to data clustering. The graph is built from a subset of the MNIST database, as a k-NNG with $k = 5$. The similarity function function is computed using two-sided tangent distance and the velocity is defined according to (6.9) where F as in the Chan-Vese model. Each cluster is represented by a front, randomly initialized.

7.3.4 High dimensional semi-supervised data classification

In this last experiment, we have tested the performance of our proposed framework when applied to semi-supervised classification on three standard databases from the literature: MNIST [26], OPTDIGITS [3], and PENDIGITS [2]. We compare two kinds of velocities. The first one is that of active contours (6.9) (denoted as AC). The second one is propagation using the Eikonal evolution equation on graphs (6.13) (denoted as EE). For these databases we merged both the training and the test sets (as performed in [6]), resulting in datasets of 70000 instances, 5620 instances, and 10992 instances, for MNIST, OPTDIGITS, and PENDIGITS, respectively. In our tests, we propose also, to refine the classification results of EE with AC algorithms. The refinement consists in applying EE with an initial condition, and then applying AC with the output of EE as an initial condition. The corresponding result will be coined EE+AC. In Table 1, we compare the performance of these three methods in terms of classification accuracy. We vary the amount of initial seeds (pre-labeled data) from 1% to 10%, and compute the average classification accuracy over 10 runs of each algorithm.

seeds	datasets	EE	AC	EE+AC
1%	MNIST	97.45%	98.20%	98.24%
	OPTDIGITS	95.22%	96.82%	97.10%
	PENDIGITS	95.75%	95.71%	96.25%
2%	MNIST	97.64%	98.24%	98.29%
	OPTDIGITS	97.41%	97.88%	97.92%
	PENDIGITS	97.38%	97.06%	98.56%
5%	MNIST	97.95%	98.33%	98.37%
	OPTDIGITS	98.09%	98.38%	98.35%
	PENDIGITS	98.25%	98.30%	98.56%
10%	MNIST	98.19%	98.39%	98.45%
	OPTDIGITS	98.41%	98.64%	98.51%
	PENDIGITS	98.94%	98.92%	99.10%

Table 1: Average classification accuracy on the three datasets for the three methods.

References

[1] N. Abatangelo and E. Valdinoci. A notion of nonlocal curvature. *Numerical Functional Analysis and Optimization*, 35(7-9):793–815, 2014.

[2] F. Alimoğlu and E. Alpaydin. Combining multiple representations for pen-based hand-written digit recognition. *Turkish Journal of Electrical Engineering & Computer Sciences*, 9(1):1–12, 2001.

[3] E. Alpaydin and C. Kaynak. Optical recognition of handwritten digits, uci machine learning repository, 1998.

[4] L. Ambrosio, G. De Philippis, and L. Martinazzi. Gamma-convergence of nonlocal perimeter functionals. *Manuscripta Mathematica*, 134(3-4):377–403, 2011.

[5] J. Bourgan, H. Brezis, and P. Mironescu. Another look at sobolev spaces. In *Optimal control and partial differential equation. Conference*, pages 439–455, 2001.

[6] X. Bresson, T. Laurent, D. Uminsky, and J. H. Von Brecht. Multiclass total variation clustering. *arXiv preprint arXiv:1306.1185*, 2013.

[7] H. Brezis. How to recognize constant functions. connections with sobolev spaces. *Russian Mathematical Surveys*, 57(4):693, 2002.

[8] B. Buet, J.-M. Mirebeau, Y. van Gennip, F. Desquilbet, J. Dreo, F. Barbaresco, G. P. Leonardi, S. Masnou, and C.-B. Schönlieb. Partial differential equations and variational methods for geometric processing of images. *The SMAI journal of computational mathematics*, 5:109–128, 2019.

[9] T. Bühler and M. Hein. Spectral clustering based on the graph p-Laplacian. In *Proceedings of the 26th Annual International Conference on Machine Learning*, ICML '09, pages 81–88, New York, NY, USA, 2009. ACM.

[10] M. Burger, A. C. Mennucci, S. Osher, and M. Rumpf. *Level Set and PDE Based Reconstruction Methods in Imaging: Cetraro, Italy 2008, Editors: Martin Burger, Stanley Osher*, volume 2090. Springer, 2013.

[11] L. Caffarelli, J.-M. Roquejoffre, and O. Savin. Nonlocal minimal surfaces. *Communications on pure and applied mathematics*, 63(9):1111–1144, 2010.

[12] L. Caffarelli and E. Valdinoci. Uniform estimates and limiting arguments for nonlocal minimal surfaces. *Calculus of Variations and Partial Differential Equations*, 41(1-2):203–240, 2011.

[13] A. Chambolle, M. Morini, and M. Ponsiglione. Nonlocal curvature flows. *Archive for Rational Mechanics and Analysis*, 218(3):1263–1329, 2015.

[14] A. Chambolle and T. Pock. Approximating the total variation with finite differences or finite elements, 2021.

[15] T. F. Chan and L. A. Vese. Active contours without edges. *IEEE Transactions on image processing*, 10(2):266–277, 2001.

[16] J. Dávila. On an open question about functions of bounded variation. *Calculus of Variations and Partial Differential Equations*, 15(4):519–527, 2002.

[17] X. Desquesnes, A. Elmoataz, and O. Lézoray. Eikonal equation adaptation on weighted graphs: fast geometric diffusion process for local and non-local image and data processing. *Journal of Mathematical Imaging and Vision*, 46(2):238–257, 2013.

[18] X. Desquesnes, A. Elmoataz, O. Lézoray, and V.-T. Ta. Efficient algorithms for image and high dimensional data processing using eikonal equation on graphs. In *International Symposium on Visual Computing*, pages 647–658. Springer, 2010.

[19] A. El Chakik, A. Elmoataz, and X. Desquesnes. Mean curvature flow on graphs for image and manifold restoration and enhancement. *Signal processing*, 105:449–463, 2014.

[20] A. Elmoataz, X. Desquesnes, and O. Lézoray. Non-local morphological pdes and p-Laplacian equation on graphs with applications in image processing and machine learning. *IEEE Journal of Selected Topics in Signal Processing*, 6(7):764–779, 2012.

[21] A. Elmoataz, O. Lezoray, and S. Bougleux. Nonlocal discrete regularization on weighted graphs: a framework for image and manifold processing. *IEEE transactions on Image Processing*, 17(7):1047–1060, 2008.

[22] A. Elmoataz, M. Toutain, and D. Tenbrinck. On the p-Laplacian and ∞-Laplacian on graphs with applications in image and data processing. *SIAM Journal on Imaging Sciences*, 8(4):2412–2451, 2015.

[23] L. J. Grady and J. R. Polimeni. *Discrete calculus: Applied analysis on graphs for computational science*. Springer Science & Business Media, 2010.

[24] L. Hagen and A. B. Kahng. New spectral methods for ratio cut partitioning and clustering. *IEEE transactions on computer-aided design of integrated circuits and systems*, 11(9):1074–1085, 1992.

[25] D. Keysers, J. Dahmen, T. Theiner, and H. Ney. Experiments with an extended tangent distance. In *Proceedings 15th International Conference on Pattern Recognition. ICPR-2000*, volume 2, pages 38–42. IEEE, 2000.

[26] Y. LeCun and C. Cortes. The mnist database of handwritten digits. *URL http://yann.lecun.com/exdb/mnist*, 2010.

[27] R. Malladi and J. A. Sethian. Image processing: Flows under min/max curvature and mean curvature. *Graphical models and image processing*, 58(2):127–141, 1996.

[28] J. M. Mazón, J. D. Rossi, and J. Toledo. *Nonlocal Perimeter, Curvature and Minimal Surfaces for Measurable Sets*. Frontiers in Mathematics. Birkhäuser, 2019.

[29] J. M. Mazón, M. Solera, and J. Toledo. The total variation flow in metric random walk spaces. *Calculus of Variations and Partial Differential Equations*, 59(1):1–64, 2020.

[30] D. B. Mumford and J. Shah. Optimal approximations by piecewise smooth functions and associated variational problems. *Communications on pure and applied mathematics*, 1989.

[31] S. Osher and R. Fedkiw. *Level set methods and dynamic implicit surfaces*, volume 153. Springer Science & Business Media, 2006.

[32] L. I. Rudin, S. Osher, and E. Fatemi. Nonlinear total variation based noise removal algorithms. *Physica D: nonlinear phenomena*, 60(1-4):259–268, 1992.

[33] F. Schulze. Evolution of convex hypersurfaces by powers of the mean curvature. *Mathematische Zeitschrift*, 251(4):721–733, 2005.

[34] J. A. Sethian. *Level set methods and fast marching methods: evolving interfaces in computational geometry, fluid mechanics, computer vision, and materials science*, volume 3. Cambridge university press, 1999.

[35] J. Shi and J. Malik. Normalized cuts and image segmentation. *IEEE Transactions on pattern analysis and machine intelligence*, 22(8):888–905, 2000.

[36] P. Y. Simard, Y. A. LeCun, J. S. Denker, and B. Victorri. Transformation invariance in pattern recognition, tangent distance and tangent propagation. In *Neural networks: tricks of the trade*, pages 239–274. Springer, 1998.

[37] A. Szlam and X. Bresson. Total variation, cheeger cuts. In *ICML*, 2010.

[38] V.-T. Ta, A. Elmoataz, and O. Lézoray. Nonlocal pdes-based morphology on weighted graphs for image and data processing. *IEEE transactions on Image Processing*, 20(6):1504–1516, 2010.

[39] J.-P. Tillich. Edge isoperimetric inequalities for product graphs. *Discrete Mathematics*, 213(1-3):291–320, 2000.

[40] Y. Van Gennip, N. Guillen, B. Osting, and A. L. Bertozzi. Mean curvature, threshold dynamics, and phase field theory on finite graphs. *Milan Journal of Mathematics*, 82(1):3–65, 2014.

[41] L. A. Vese and T. F. Chan. A multiphase level set framework for image segmentation using the mumford and shah model. *International journal of computer vision*, 50(3):271–293, 2002.

[42] U. Von Luxburg. A tutorial on spectral clustering. *Statistics and computing*, 17(4):395–416, 2007.